Diurnal and seasonal variation of electron heat flux measured with the Poker Flat Incoherent-Scatter Radar

Christopher T. Fallen[1] and Brenton J. Watkins[2]

[1]   Measurements made with the Advanced Modular Incoherent Scatter Radar were used to calculate the average diurnal electron temperature and corresponding vertical heat flux above Poker Flat, Alaska. Our results show that both the electron heat flux and temperature exhibited seasonal variation during 12 consecutive months in 2009 and 2010, a period of exceptionally quiet solar and geomagnetic activity. Both the electron temperature and heat flux varied diurnally, with larger magnitudes observed during the day than night. Contrary to midlatitude measurements from the late 1960s, the downward heat fluxes above Poker Flat were found to vary significantly with season and were typically greater during summer than winter. The time-dependent topside electron heat flux is an important parameter describing magnetosphere-ionosphere coupling and it also drives boundary conditions in physics-based ionosphere models. Parameterizations of the average electron thermal flux and temperature sufficient for use in ionosphere models are provided. A physics-based high-latitude ionosphere model is used to demonstrate that a constant heat flux boundary condition leads to an electron temperature increase near local midnight that is not observed in the radar measurements. The resulting inaccuracy in electron temperature calculations leads to more than a 15% overestimate of daytime peak electron number density. Applying a time-varying heat flux boundary condition brings the model electron temperature and peak density to good agreement with measurements.

1.   Introduction

[2]   Conductive heat flux between the magnetosphere and ionosphere through the electron gas is not a well-understood quantity even though it significantly influences electron temperatures in the F_2 region ionosphere and is an important parameter used in several physics-based ionosphere models. The electron gas in the ionosphere and magnetosphere transfers heat primarily through Coulomb collisions with charged particles, and also through electron-neutral collisions in the E and lower F regions. Photoelectron escape from geomagnetic conjugate points provides a possible mechanism for maintaining a plasmaspheric heat source that supplies heat to the midlatitude F_2 region ionosphere. In the high-latitude ionosphere, the interaction between escaping electrons with the solar wind is a potential source of downward-conducting heat (see *Newell et al.* [2009] for a review of polar cap particle precipitation).

[3]   Early incoherent scatter radar (ISR) measurements of the midlatitude ionosphere indicated a positive vertical electron temperature gradient that, in the absence of significant heat sources or sinks in the F_2 region, implies a downward (geomagnetic field aligned) heat flow from the magnetosphere [*Evans*, 1967]. By matching model electron temperature profiles to ISR-measured profiles, *Evans and Mantas* [1968] estimated the magnitude of the autumn daytime electron thermal flux to be $\sim 8\ \mu W/m^2$ at 1000 km altitude above Millstone Hill, Massachusetts. The seasonal variation of the daytime electron heat flux over Millstone Hill was observed to vary from approximately 3 to 10 $\mu W/m^2$ at 500 km altitude, while the corresponding nighttime electron heat flux varied from 1 to 5 $\mu W/m^2$. In both cases, the minimum occurred during local summer and the maximum occurred during winter [*Evans*, 1967]. These observations remained consistent through multiple ISR campaigns at Millstone Hill and Saint-Santin, France [*Taylor and McPherson*, 1974], with the magnitude of the downward flux showing some dependence on sunspot activity [*Evans*, 1973a, 1973b].

[4]   In the high-latitude ionosphere, *Rasmussen et al.* [1988] used measurements made with the radar at Chatanika, Alaska and model runs to infer a summertime downward heat flux at 1000 km altitude and it was found to vary diurnally from 0 to 11 $\mu W/m^2$. *Blelly and Alcayde* [1994] measured the diurnally varying heat flux at 400 km altitude during summer and winter

---

Additional supporting information may be found in the online version of this article.

[1]Arctic Region Supercomputing Center, University of Alaska Fairbanks, Fairbanks, Alaska, USA.

[2]Geophysical Institute, University of Alaska Fairbanks, Fairbanks, Alaska, USA.

Corresponding author: C. T. Fallen, Arctic Region Supercomputing Center, University of Alaska Fairbanks, 909 Koyukuk Dr., Ste. 105, PO Box 756020, Fairbanks, AK 99775-6020, USA. (ctfallen@alaska.edu)
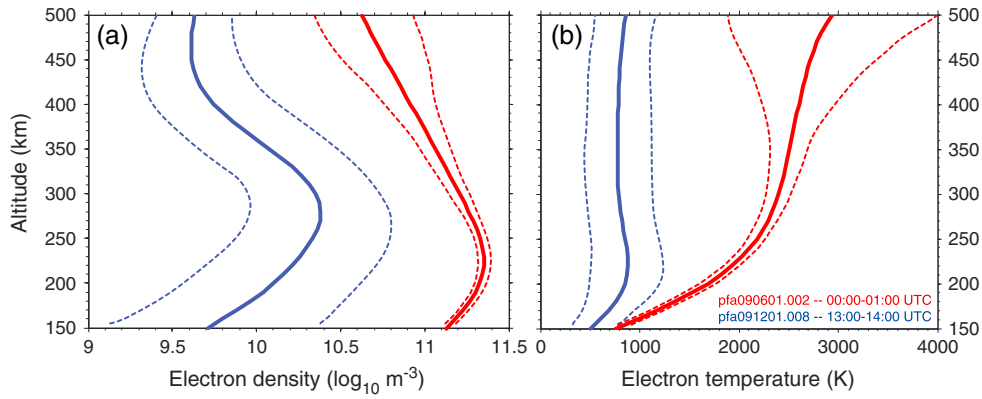
Figure 1. Fitted profiles of (a) electron density and (b) electron temperature with error estimates for typical best-case and worst-case measurement conditions. Solid blue curves fitted to measurements from worst-case conditions from 12:00 to 13:00 UTC collected between 1 December 2009 and 1 January 2010 and solid red curves are fitted to best-case measurements from 00:00 to 01:00 UTC collected between 1 June and 1 July 2009. Dashed curves indicate the standard deviation of the binned measurements at each altitude.

with the European Incoherent Scatter (EISCAT)-VHF radar and reported a downward late springtime heat flux of 20 μW/m^2 during the day and 10 μW/m^2 around midnight, decreasing to 3 μW/m^2 and 0.5 μW/m^2 during midwinter daytime and nighttime, respectively. A detailed statistical analysis of EISCAT-UHF electron temperature measurements by *Breen et al.* [1996] confirmed that, similar to midlatitude electron thermal flux, the daytime high-latitude flux varies with sunspot activity. At 300 km altitude, the downward daytime heat flux varied from 10 μW/m^2 with an $S_{10.7}$ Covington index of 50 to a heat flux of 16 μW/m^2 with an $S_{10.7}$ of 250. (The $S_{10.7}$ solar index is described by *Tobiska et al.* [2008].) After adjusting for solar activity, no apparent seasonal variation was observed. Interestingly, *Breen et al.* [1996] observed the downward heat flux to increase with altitude, contrasting with the altitude dependence inferred by *Blelly and Alcayde* [1994] and *Rasmussen et al.* [1988].

[5] *Bekerat et al.* [2007] used in situ Defense Meteorological Satellite Program (DMSP) measurements from 1998 with model calculations of plasma density to infer the electron thermal flux above the polar cap. Their model electron density results were found to best fit the DMSP observations when a diurnally constant downward heat flux was assumed in the model which varied seasonally from 8.0 to 24 μW/m^2 at 840 km altitude. Compared with the midlatitude ionosphere, relatively little is known about magnetosphere-ionosphere thermal flows in the polar cap.

[6] In this paper, we report the average diurnal variation of the electron thermal flux and temperature at 350 km altitude above Poker Flat, Alaska. The thermal flux was estimated from Advanced Modular Incoherent Scatter Radar (AMISR) measurements of electron density and temperature with a low-duty cycle International Polar Year (IPY) mode [*Sojka et al.*, 2009]. The continuous operation of this facility has enabled a new capability to study the seasonal behavior of thermal flux in the auroral zone. Diurnal-periodic time series of electron thermal flux and temperature suitable for use in ionosphere models were constructed for this study for each month from June 2009 through May 2010.

2. ISR Measurements

[7] The vertical electron thermal flux ϕ_e in the high-latitude ionosphere may be written as a function of electron thermal conductivity λ_e, the vertical electron temperature gradient, and the geomagnetic dip angle I

$$\phi_e = -\lambda_e \frac{\partial T_e}{\partial z} \sin^2 I. \qquad (1)$$

[8] *Banks* [1966] provides an approximate expression for thermal conductivity in the E and F regions which is a function of electron temperature and electron number density. Therefore, the electron thermal flux may be estimated from ISR measurements of electron density and temperature over a range of altitudes. However, ISR-measured profiles above the F_2 peak layer are typically noisy and vary with time, making it difficult to estimate the electron temperature gradient in (1) without averaging.

[9] Long-duration measurements of electron density and temperature from the Poker Flat Incoherent Scatter Radar (PFISR) were binned according to UTC hour to construct average time-dependent electron density and temperature profiles. PFISR has operated nearly continuously in a low-duty cycle since the start of the International Polar Year (IPY) on 1 March 2007. IPY mode measurements from 1 June 2009 through 31 May 2010 have been used for this study. The data consist of 12 sequential "IPY17" experiments with start and end dates corresponding approximately to the first and last day of each month. PFISR transmitted interleaved pulses in four directions including vertical and magnetic zenith. F-region electron density and temperature estimates are based on 480 μs long-pulse data. (see *Sojka et al.* [2009, and references therein] for further details on the radar pulse modulation and measurement techniques.) Each monthly data set contained between 5000 and 10,000 measured profiles; each 1 h data bin contained approximately 200 to 400 electron density and temperature profiles with 17 range bins covering altitudes between 122 and 673 km. Antenna direction information was discarded; the data in
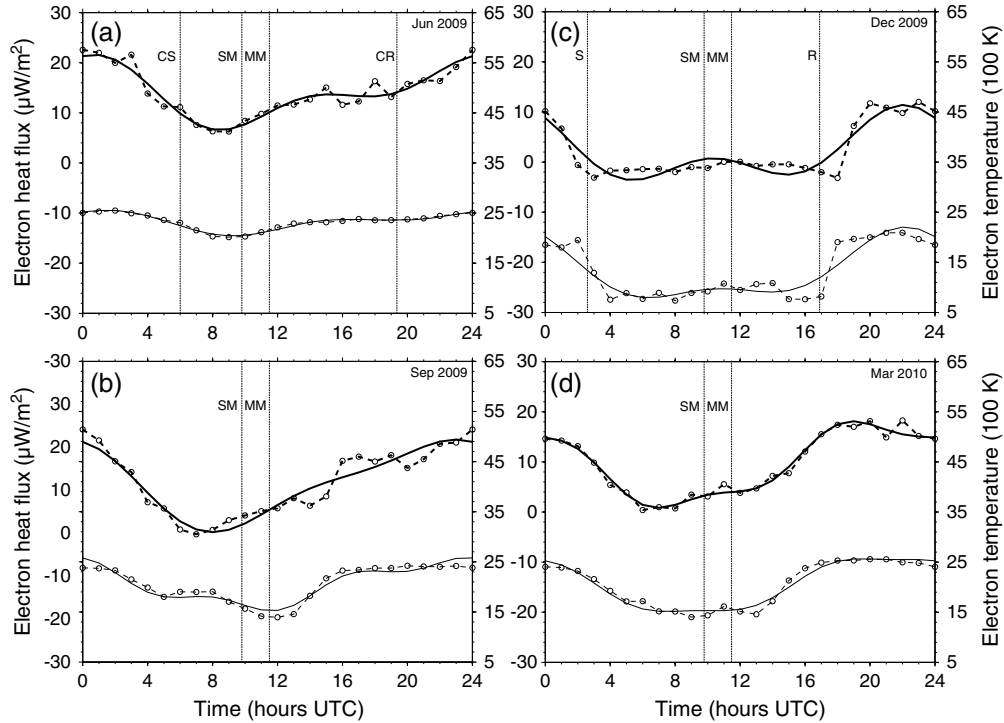
Figure 2. Functions of vertical electron thermal flux (bold curve) and temperature at 350 km altitude above Poker Flat, Alaska during (a) June 2009, (b) September 2009, (c) December 2009, and (d) March 2010. Data points from average monthly altitude profiles are plotted as open circles. Solar midnight (SM) and magnetic midnight (MM) are labeled in each panel. Vertical lines indicate local sunrise/sunset (R, S) and conjugate sunrise/sunset (CR, CS) times on the 15th of each month at 200 km altitude. On 15 September and March, the atmosphere at 200 km altitude above Poker Flat and its conjugate point is continuously sunlit.

each bin consisted of ordered triples (z, $n_e(z)$, $T_e(z)$) of altitude, electron number density, and electron temperature.

[10] To construct smooth density and temperature profiles, order-10 polynomials were fit to (z, $\log_{10} n_e$) and (z, T_e) ordered pairs from each bin which minimized the respective sums of the squares of the residuals (least squares fit). The polynomial fits did not appear to be sensitive to small changes in the polynomial order nor to the omission of small random sets of data points. Figure 1 shows representative fitted polynomial curves of electron density and temperature data during typical best-case (summer afternoon) and worst-case (winter evening) ISR measurement conditions. The standard deviation of the binned measurements at each altitude is indicated by the dashed fitted curves. While measurement quality is generally poor during worst-case conditions, particularly the electron density measurements, the effect on the thermal flux calculations from (1) is limited since the electron temperature gradient is typically small during winter evenings.

[11] Time series of electron thermal flux $\phi_e(t)$ and temperature $T_e(t)$ were created for each month by evaluating the polynomial profiles and their derivatives at a constant altitude and substituting the values into (1). In general, evaluation of the electron conduction coefficient λ_e from *Banks* [1966] requires number density estimates of the neutral gas constituents. These values were obtained from the US Naval Research Laboratory mass spectrometer and incoherent scatter radar (NRLMSISE-00) model [*Picone et al.*, 2002], but at 350 km

altitude, the thermal conductivity expression for a fully ionized plasma $\lambda_e \approx 7.7 \times 10^5 \, T_e^{5/2}$ eV cm^{-1} s^{-1} K^{-1} may be used without loss of generality. Also note that the classical electron thermal conductivity expression used here from *Banks* [1966] should be corrected by a factor or 0.42, as demonstrated by *Blelly and Schunk* [1993] and *Blelly and Alcayde* [1994], to account for electron-ion collisional effects. These thermal flux results can similarly be corrected by the same factor.

[12] Each time series has 24 points and sample rate of $f_s = (1 \, h)^{-1}$. A 24 h periodic function was fit to each resulting time series of electron thermal flux and temperature with Fourier analysis. The 24 point Discrete Fourier Transform was used to approximate each time series as a linear combination of sine and cosine trigonometric functions that best fits the data in the least squares sense. That is, the thermal flux was approximated by the function

$$\phi_e(t) \approx \frac{1}{24} \sum_{k=0}^{23} [a_k \cos(2\pi k t/24) + b_k \sin(2\pi k t/24)], \, t \in \{0, 1, \cdots, 23\}$$

(2)

where the coefficients a_k and b_k together form the discrete Fourier amplitudes corresponding to frequency $f_k = k f_s/2$. All but the five largest contributing frequency components in the sum (2) for each time series were discarded. The size ranking of the largest five amplitudes was identical for the fitted temperature and flux time series for all 12 months.

[13] Figure 2 shows both the measured and fitted time series of electron thermal flux and temperature during the solstice and equinox months from June 2009 through May 2010. Vertical lines in the December and June plots indicate approximate sunrise and sunset times at 200 km above Poker Flat and its geomagnetic conjugate point, near peak photoproduction altitudes. Data Set S1 (supporting information) provides the Fourier amplitude coefficients a_k and b_k from equation (2) for reproducing the fitted curves of electron thermal flux and temperature for months June 2009 through May 2010.

[14] In each month, the downward thermal flux reached a maximum during the day and a minimum at night, consistent with a magnetospheric heat source maintained by ionospheric photoelectrons [*Evans*, 1967]. The magnitude and diurnal dependence of the downward thermal flux measurements are in general agreement with estimates by *Schunk et al.* [1986]. Note that the 350 km thermal flow appears to be directed upward for several hours before local midnight from September 2009 through January 2010. However, it is not clear that the nighttime measurements may be considered as topside thermal flows primarily because the heat flux calculations are uncertain when the ISR data are noisy, most often occurring at night when the plasma density is low.

[15] Estimating the uncertainty of the monthly average diurnal electron heat flux and temperature derived from the IPY17 long-duration ISR measurements is not straightforward to do with rigor for the multistep averaging and fitting procedure used in this study. The ISR measurements themselves contain uncertainty in addition to natural ionosphere variability over the course of each month. Nevertheless, reasonable bounds on the heat flux uncertainty may be estimated from (1) and the electron temperature error profiles illustrated in Figure 1. Electron thermal conductivity λ_e is proportional to $T_e^{5/2}$ in a fully ionized plasma, so at 350 km altitude during best-case summer daytime conditions, the uncertainty in the electron temperature is less than 10%. Uncertainty in the temperature gradient is approximately 80%, as estimated by half the difference between the gradients of the average temperature less the estimated error and the temperature plus the error. Therefore, the summer daytime electron heat flux may need a corrective factor of 2 when used to model ionospheric conditions for a particular day. A similar calculation for winter nighttime conditions (where in contrast with the summer daytime conditions, the gradient uncertainty is less than the uncertainty in temperature), a corrective factor of up to 2.5 may be appropriate.

[16] Auroral precipitation is another potential source of variability in the nighttime measurements. This precipitation takes many forms (see *Paschmann et al.* [2002] for a review) and it sometimes persists for hours after a substorm [*Jones et al.*, 2011]. Some of that energy is deposited in the F region, as can be inferred from observations of tall rays. Much of the energy transferred by auroral electrons to the ionosphere is absorbed in the E region where electron thermal conductivities are low. Auroral activity is not expected to significantly affect these climatological calculations due to the long-term (1 month) averaging technique used. Upward heat flux from auroral heat deposition will be indicated by an increase in upward 250 km heat flux (not shown) and that was not apparent in these results.

[17] With the possible exception of months near the solstices, no clear relationship between the thermal flux above Poker Flat and the (200 km) sunrise or sunset times at the conjugate point is apparent, in apparent contrast with prior midlatitude observations by *Taylor and McPherson* [1974]. In summer months when the high-latitude ionosphere is continuously sunlit at local solar midnight, the downward thermal flux steadily increases for several hours to a plateau of 14 $\mu W/m^2$ which lasts until sunrise at the conjugate ionosphere when the flux begins to increase again to a peak of approximately 22 $\mu W/m^2$. This occurs near noon solar local time (approximately 21:50 UTC) and will tend to obscure any heating effects from conjugate photoelectrons.

[18] The data have been statistically ordered in terms of UTC, and all data relate to one location (i.e., Poker Flat, Alaska) for each month. This approach is applicable for understanding average responses to both local solar effects and ionosphere-magnetosphere coupling effects for the particular solar conditions applicable to the data periods used. However, it should be emphasized that numerous geophysical conditions may result in departures from the data values shown in this paper. For example, in the auroral zone such as Poker Flat, Alaska conditions typically associated with a midlatitude type ionosphere occur during the daytime when the local ionosphere is connected to closed magnetosphere field lines. During the evening, the field lines may become open with likely quite different heat flux values. This effect is dependent on solar activity, and we therefore suggest that a larger future database could be used to derive a dependence on the magnetic Kp index, or interplanetary magnetic field, that relate to the size of the auroral oval. Another aspect that should be used in future work is a dependence on solar zenith angle. Averaging data over time sequences even over relatively short monthly periods as we have done, and with the 1 h binning of data, tends to diminish the sharp variations in heat flow associated with sunrise and sunset; this could be further examined in future studies.

[19] A clear seasonal variation is apparent in the maximum and minimum downward heat flux of each diurnal cycle. Generally, the maximum flux was approximately a factor of 2 larger in the summer compared to the winter, and the minimum heat flux in the summer is approximately equal to the maximum winter heat flux. Solar activity, as measured by average sunspot number or $F_{10.7}$ radio flux, remained very low during the time period. The $F_{10.7}$ index trended slightly upward from about 70 in June 2009 to about 82 in May 2010. No overall trend is apparent in the thermal flux results. Both the observed seasonal thermal flux variation and lack of apparent relationship with sunspot activity differ from the respective midlatitude characteristics observed by *Evans* [1973b], but the time period in this study exhibited much less solar variation, so no correlation is expected.

[20] The measurements of electron density and temperature made with the AMISR facility at Poker Flat shown here are useful for calculating the downward electron thermal flux, an important parameter for high-latitude physics-based ionosphere models and for understanding the thermal energy coupling between the magnetosphere and ionosphere. Future AMISR surveys should include simultaneous measurements from the Poker Flat and Resolute Bay facilities to better estimate the latitude dependence and variability of electron thermal flux through the high-latitude ionosphere. Long-duration
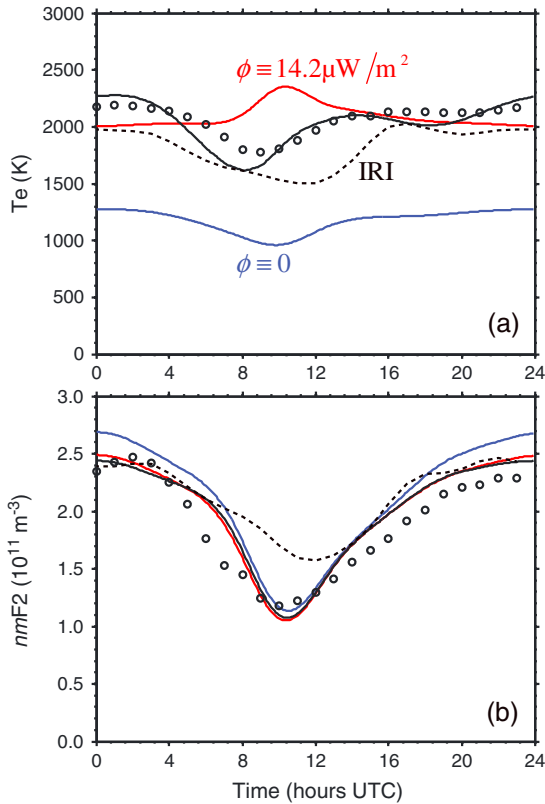
Figure 3. Average diurnal (a) 250 km electron temperature and (b) *nm*F2 above Poker Flat, Alaska during June 2009. Solid curves are calculated with a self-consistent ionosphere model using (black) the diurnally varying electron heat flux upper boundary condition shown in Figure 2, (blue) a zero-flux boundary condition, and (red) a constant boundary condition equal to the time-averaged flux. Corresponding Poker Flat ISR measurements are plotted with circles.

measurements made from both facilities at the end of the deep solar cycle minima will allow verification of thermal flux sunspot dependence observed at midlatitudes in the 1960s and 1970s. The ongoing solar maximum and consequent buildup of ionosphere plasma density will facilitate ISR measurements at higher altitudes for long-term studies of the thermal flux altitude dependence. Finally, it will be worthwhile to determine whether the apparent evening upward flows of heat during the spring are physical or are merely artifacts of noisy ISR measurements and long-duration averaging. Coordinated radar and optical campaigns could determine whether auroral processes cause upward heat flow, if any, to the magnetosphere.

3. Model and Discussion

[21] Effects of a diurnally varying downward electron thermal flux on the *F*-region ionosphere were investigated with the one-dimensional self-consistent ionosphere model (SCIM) [*Fallen et al.*, 2011]. The ionosphere model solves time-dependent ion density and momentum equations fully coupled with ion and electron energy equations in the corotating frame above Poker Flat. Neutral atmosphere parameters were provided by the NRLMSISE-00 and

horizontal wind model (HWM93) [*Hedin et al.*, 1996] empirical models. A solar ionizing spectrum was obtained from the solar EUV flux model for aeronomic calculations (EUVAC) model [*Richards et al.*, 1994]. Atomic oxygen density from Mass Spectrometer Incoherent Scatter was reduced by 50%, following the suggestion of *Milikh et al.* [2010], resulting in better agreement between the measured and observed electron density and temperature profiles.

[22] The topside simulation boundary was set at 350 km altitude, so the time-varying electron thermal flux estimated from the June 2009 PFISR measurements could be used directly as a boundary condition for the electron energy equation. One concern with placing the top boundary of a physics-based ionosphere model at such a low altitude, near the transition where local collisional processes are of equal importance as transport processes, is that the simulated ionosphere below the *F*-region peak layer may be overly influenced by the topside boundary condition. Vertical electron thermal flux in the summer ionosphere over Poker Flat was calculated to be essentially independent of altitude above 350 km in separate model runs with the top boundary set at 1000 km. Below 350 km altitude, collisional processes and upward thermal flows resulting from photoionization cause steep altitude gradients in the electron thermal flux. The calculated altitude-independence of electron thermal flux above 350 km altitude justifies the use of these heat flux results in simulations with topside boundaries at or above 350 km altitude. This assertion was further verified by comparing the peak layer plasma density, height, and temperature as functions of time calculated with two models that differed only in the choice of boundary altitude. No apparent differences were observed in calculations from models with 350 km versus 1000 km boundaries.

[23] Another concern is that it is not necessarily clear that a 1-D model can accurately simulate the vertical structure of the high-latitude ionosphere, a region frequently defined by strong horizontal convection and inhomogeneity, particularly at night. However, *Richards et al.* [2009] used long-duration PFISR measurements of electron density and temperature to validate the use of the field line interhemispheric plasma (FLIP) model for simulating the ionosphere over Poker Flat and found generally good agreement between the measurements and model results during quiet geomagnetic conditions. FLIP is also a 1-D model of the corotating ionosphere; its primary difference from SCIM is that FLIP solves the model equations along a field line to the conjugate hemisphere and does not assume a topside ionosphere boundary condition (or magnetospheric heat source). Also note that *Richards et al.* [2009] used FLIP to calculate equivalent neutral wind velocities and found that the calculated velocities agreed well with those from HWM93 which has had mixed success with reproducing neutral winds at high latitudes.

[24] Simulated electron temperature at 250 km altitude, just above the *F*-region peak altitude, is plotted as a function of time in Figure 3a for three choices of electron energy equation boundary conditions: no electron thermal flux, constant flux $\phi_e(t) \equiv 14.2 \ \mu W/m^2$ equal to the time average of the June 2009 measurements shown in Figure 2, and the time-varying ISR-measured flux. For comparison, the average 250 km electron temperature ISR measurements estimated with the process described above are plotted with the modeled temperatures. Figure 3b shows corresponding *nm*F2 calculated with the model and measured with ISR. Electron temperature and *nm*F2 calculated with International Reference Ionosphere

IRI-2007 empirical model [*Bilitza and Reinisch*, 2008] are also shown in Figure 3 for comparison. A zero-flux boundary condition causes the model to underestimate the 250 km electron temperature by approximately 800 K throughout the day. Similarly, when the boundary condition is set to the constant time-averaged flux value, the model underestimated electron temperature near local noon but overestimated temperature near local midnight. In fact, the calculated electron temperature increases in the evening due to falling electron number density while the boundary heat flux remains constant, resulting in more heating per electron. The experimentally-determined time-varying thermal flux boundary condition brings the measured and modeled 250 km electron temperatures to reasonable agreement; the model reproduces the magnitudes as well as local minima and maxima of the temperatures observed with radar. Both the constant diurnal-average flux and diurnally varying flux model runs calculate a diurnal nmF2 curve that agrees well with ISR measurements except during local sunrise and sunset, when the model tends to overestimate nmF2 by approximately 20%. The zero-flux model run overestimates daytime nmF2 by at least 15% and generally calculates electron densities larger than those from the other model runs.

[25] A constant-flux boundary condition equal to the time-average of the diurnal flux is sufficient to model daytime T_e and nmF2 in the high-latitude ionosphere, but a time-varying boundary condition is necessary to accurately reproduce night-time electron temperatures, even during the summer solstice when the ionosphere is continuously sunlit. This has implications for the high-latitude domain of models such as the National Center for Atmospheric Research Thermosphere Ionosphere Electrodynamics General Circulation Model (TIE-GCM) [*Richmond et al.*, 1992]. Version 1.94 of TIE-GCM uses an electron heat flux that is essentially constant at the Poker Flat latitude during the summer solstice (TIE-GCM v1.94 model description at http://www.hao.ucar.edu/modeling/tgcm/doc/description/model_description.pdf). Consequently, electron temperatures modeled by TIE-GCM are likely to be inaccurate at high latitudes, especially for large solar zenith angles, leading to inaccuracies in calculated nmF2.

[26] Future measurements from the Poker Flat and Resolute Bay ISR facilities during the ongoing solar maximum will allow for similar flux measurements but at higher altitudes. Future research will also verify that the correlation between solar activity and magnetospheric heat flux observed during earlier midlatitude studies also applies at high latitudes. Assimilation of long-duration measurements from Poker Flat and Resolute Bay into the boundary conditions of physics-based ionosphere models will further improve model accuracy.

References

Banks, P. (1966), Charged particle temperatures and electron thermal conductivity in the upper atmosphere, *Ann. Geophys.*, *22*, 557–587.

Bekerat, H. A., R. W. Schunk, and L. Scherliess (2007), Estimation of the high-latitude topside electron heat flux using DMSP plasma density measurements, *J. Atmos. Sol.-Terr. Phys.*, *69*(9), 1029–1048, doi:10.1016/j.jastp.2007.03.015.

Bilitza, D., and B. W. Reinisch (2008), International Reference Ionosphere 2007: Improvements and new parameters, *Adv. Space Res.*, *42*(4), 1845–1950.

Blelly, P.-L., and D. Alcayde (1994), Electron heat flow in the auroral ionosphere inferred from EISCAT-VHF observations, *J. Geophys. Res.*, *99*(A7), 1,3181–1,3188, doi:10.1029/93JA03493.

Blelly, P.-L., and R. W. Schunk (1993), A comparative study of the time-dependent standard 8-, 13-, and 16-moment transport formulations of the polar wind, *Ann. Geophys.*, *11*, 443–469.

Breen, A. R., P. J. S. Williams, A. Etemadi, and V. N. Davda (1996), Uncertainties in measurements of electron temperature and the estimation of F-region electron heat conduction from EISCAT data, *J. Atmos. Terr. Phys.*, *58*(1–4), 149–159, doi:10.1016/0021-9169(95)00026-7.

Evans, J. V. (1967), Midlatitude electron and ion temperatures at sunspot minimum, *Planet. Space Sci.*, *15*(10), 1557–1570, doi:10.1016/0032-0633(67)90089-x.

Evans, J. V. (1973a), Seasonal and sunspot cycle variations of F region electron temperatures and protonospheric heat fluxes, *J. Geophys. Res.*, *78*(13), 2344–2349, doi:10.1029/JA078i013p02344.

Evans, J. V. (1973b), Millstone Hill Thomson scatter results for 1966 and 1967, *Planet. Space Sci.*, *21*(5), 763–792, doi:10.1016/0032-0633(73)90095-0.

Evans, J. V., and G. P. Mantas (1968), Thermal structure of the temperate latitude ionosphere, *J. Atmos. Terr. Phys.*, *30*(4), 563–577, doi:10.1016/0021-9169(68)90059-7.

Fallen, C. T., J. A. Secan, and B. J. Watkins (2011), In-situ measurements of topside ionosphere electron density enhancements during an HF-modification experiment, *Geophys. Res. Lett.*, *38*, L08813, doi:10.1029/2011gl046887.

Hedin, A. E., et al. (1996), Emperical wind model for the upper, middle and lower atmosphere, *J. Atmos. Terr. Phys.*, *58*(13), 1421–1447.

Jones, S. L., M. R. Lessard, K. Rychert, E. Spanswick, and E. Donovan (2011), Large-scale aspects and temporal evolution of pulsating aurora, *J. Geophys. Res.*, *116*, A03214, doi:10.1029/2010ja015840.

Milikh, G. M., A. G. Demekhov, K. Papadopoulos, A. Vartanyan, J. D. Huba, and G. Joyce (2010), Model for artificial ionospheric duct formation due to HF heating, *Geophys. Res. Lett.*, *37*, L07803, doi:10.1029/2010gl042684.

Newell, P. T., K. Liou, and G. R. Wilson (2009), Polar cap particle precipitation and aurora: Review and commentary, *J. Atmos. Sol.- Terr. Phys.*, *71*(2), 199–215.

Paschmann, G., S. Haaland, and R. Treumann (2002), Auroral plasma physics, *Space Sci. Rev.*, *103*(1–4), 1–485.

Picone, J. M., A. E. Hedin, D. P. Drob, and A. C. Aikin (2002), NRLMSISE-00 empirical model of the atmosphere: Statistical comparisons and scientific issues, *J. Geophys. Res.*, *107*(A12), 1468, doi:10.1029/2002JA009430.

Rasmussen, C. E., J. J. Sojka, R. W. Schunk, V. B. Wickwar, and O. de La Beaujardiere (1988), Comparison of simultaneous Chatanika and Millstone Hill temperature measurements with ionospheric model predictions, *J. Geophys. Res.*, *93*, 1922–1932, doi:10.1029/JA093iA03p01922.

Richards, P. G., J. A. Fennelly, and D. G. Torr (1994), EUVAC: A solar EUV flux model for aeronomic calculations, *J. Geophys. Res.*, *99*(A5), 8981–8992, doi:10.1029/94ja00518.

Richards, P. G., M. J. Nicolls, C. J. Heinselman, J. J. Sojka, J. M. Holt, and R. R. Meier (2009), Measured and modeled ionospheric densities, temperatures, and winds during the international polar year, *J. Geophys. Res.*, *114*, A12317, doi:10.1029/2009ja014625.

Richmond, A. D., E. C. Ridley, and R. G. Roble (1992), A thermosphere/ionosphere general circulation model with coupled electrodynamics, *Geophys. Res. Lett.*, *19*(6), 601–604, doi:10.1029/92gl00401.

Schunk, R. W., J. J. Sojka, and M. D. Bowline (1986), Theoretical study of the electron temperature in the high-latitude ionosphere for solar maximum and winter conditions, *J. Geophys. Res.*, *91*(A11), 12,041–12,054, doi:10.1029/JA091iA11p12041.

Sojka, J. J., M. J. Nicolls, C. J. Heinselman, and J. D. Kelly (2009), The PFISR IPY observations of ionospheric climate and weather, *J. Atmos. Sol.- Terr. Phys.*, *71*(6–7), 771–785, doi:10.1016/j.jastp.2009.01.001.

Taylor, G. N., and P. H. McPherson (1974), Diurnal and seasonal variations of exospheric heat flux at a mid-latitude station, *J. Atmos. Terr. Phys.*, *36*(7), 1135–1146, doi:10.1016/0021-9169(74)90102-0.

Tobiska, W. K., S. D. Bouwer, and B. R. Bowman (2008), The development of new solar indices for use in thermospheric density modeling, *J. Atmos. Sol.-Terr. Phys.*, *70*(5), 803–819, doi:10.1016/j.jastp.2007.11.001.